



Marini, Daniele and Corney, Jonathan (2017) A methodology for assessing the feasibility of producing components by flow forming. *Production and Manufacturing Research*, 5 (1). pp. 210-234. ISSN 2169-3277 , <http://dx.doi.org/10.1080/21693277.2017.1374888>

This version is available at <https://strathprints.strath.ac.uk/62002/>

Strathprints is designed to allow users to access the research output of the University of Strathclyde. Unless otherwise explicitly stated on the manuscript, Copyright © and Moral Rights for the papers on this site are retained by the individual authors and/or other copyright owners. Please check the manuscript for details of any other licences that may have been applied. You may not engage in further distribution of the material for any profitmaking activities or any commercial gain. You may freely distribute both the url (<https://strathprints.strath.ac.uk/>) and the content of this paper for research or private study, educational, or not-for-profit purposes without prior permission or charge.

Any correspondence concerning this service should be sent to the Strathprints administrator: strathprints@strath.ac.uk

A methodology for assessing the feasibility of producing components by flow forming

Daniele Marini  and Jonathan Corney

Department of Design, Manufacture & Engineering Management (DMEM), University of Strathclyde, Glasgow, UK

ABSTRACT

This paper describes a methodology for assessing the applicability of the flow forming process for the manufacture of specific components. The process starts by filtering potential candidates for flow forming from a component collection and then carries out a detailed assessment of quantitative, technological and economic feasibility before determining a viable process plan. The process described uses analytical relationships and criteria drawn from the literature. For example, qualitative feasibility is evaluated using analytical relationships for ultimate strength prediction. Similarly technological validation is done estimating forming process forces and defects rate which are evaluated against threshold values. A process time model is used to develop a hybrid cost model in order to evaluate economic feasibility. Using these calculated values production feasibilities are established by comparison with reported reduction ratios and process parameters. The paper concluded with a brief summary of the results of applying the process to an industrial case study.

ARTICLE HISTORY

Received 15 December 2016
Accepted 28 February 2017

KEYWORDS

Flow forming; process modeling; analytical prediction; manufacturing framework; feasibility methodology

1. Introduction

Essentially flow forming is a deformation process carried out by rollers that compresses and stretches a blank (called a preform) over a rotating mandrel, usually in a number of consecutive stages (Figure 1). The appearance of heavy duty CNC flow forming machines has provided both the capability (i.e. power) to fulfill small-medium batches and a flexibility which allows production of a wide range of rotational shapes and near-net-shape components. The process is very efficient in terms of material usage and its adoption often allows reduction of component's weight and costs (both important considerations in many industrial applications) (Marini, Cunningham, & Corney, 2015).

Existent investigation on flow forming has been carried out with experimental and theoretical methodologies (analytical and numerical). In flow forming, empirical studies have been used to seek to correlations between inputs (e.g. the workpiece material's properties and process parameters such as the radial, tangential and axial forces on the

CONTACT Daniele Marini  daniele.marini@strath.ac.uk, daniele.marini19@gmail.com

© 2017 The Author(s). Published by Informa UK Limited, trading as Taylor & Francis Group.

This is an Open Access article distributed under the terms of the Creative Commons Attribution License (<http://creativecommons.org/licenses/by/4.0/>), which permits unrestricted use, distribution, and reproduction in any medium, provided the original work is properly cited.

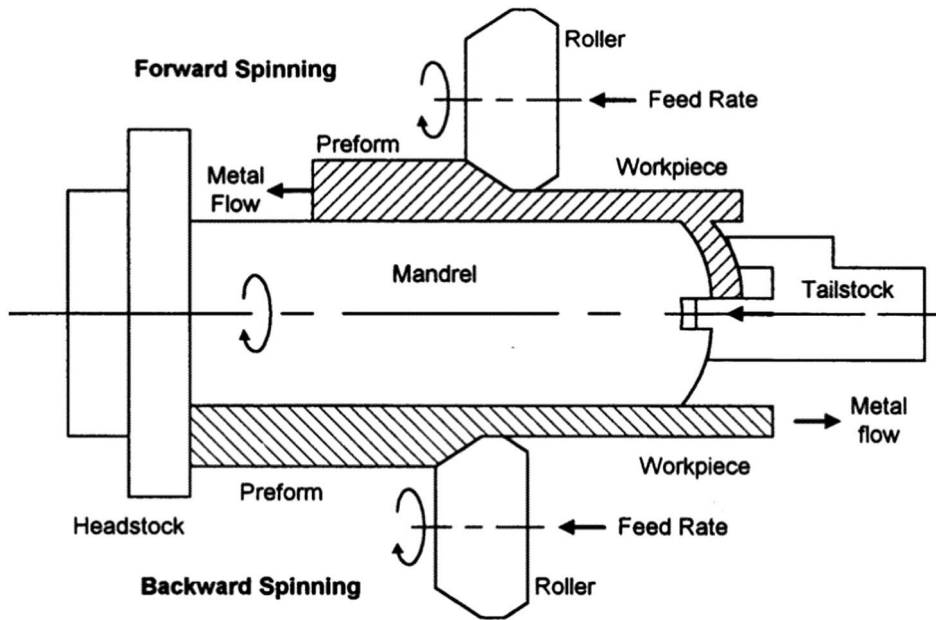


Figure 1. A schematic illustration of flow forming (Chang et al., 1998).

rollers) and outputs (e.g. surface roughness, mechanical properties or dimensional accuracy) (Marini, Cunningham, Xirouchakis, & Corney, 2016). Notable examples include (Davidson, Balasubramanian, & Tagore, 2008; Gupta, Ghosh, Kumar, Karthikeyan, & Sinha, 2007; Hayama & Kudo, 1979b; Jahazi & Ebrahimi, 2000; Podder, Mondal, Ramesh Kumar, & Yadav, 2012; Rajan, Deshpande, & Narasimhan, 2002b; Singhal, Das, & Prakash, 1987). Existent design of experiment application to flow forming process can be found in (Marini et al., 2016).

The main focus of analytical research is to develop a model of the flow of the metal during the flow forming process. This would provide the means to quantify the working energies and the forces required to form a specific geometry from a given billet. This can also give general feasibility boundaries for the process (e.g. the maximum reduction ratio achievable in one pass for a certain kind of process and metals). All the models start with the assumption of 'conservation of volume' and consequently evaluate its distribution between axial growing and radial reduction. Energy based models (Hayama & Kudo, 1979a; Jolly & Bedi, 2010; Molladavoudi & Djavanroodi, 2010; Singhal, Saxena, & Prakash, 1990) and upper-bound models (Gur & Tirosh, 1982; Mohan & Misra, 1970; Nagarajan, Kotrappa, Mallanna, & Venkatesh, 1981; Park, Kim, & Bae, 1997; Roy, Maijer, Klassen, Wood, & Schost, 2010) are the commonly used in this approach.

Finite element models (FEM) allow aspects of the flow forming process to be evaluated that are impossible to assess analytically (e.g. roller deformation). Numerical simulation avoids the expense of experiments and allows precise understandings of process trade-offs to be developed. However the implicit necessity of 3-dimensional modeling and complexity of contact surfaces create difficulties in this kind of approach. Despite this, eleven papers have reported numerical models for flow forming. Three papers use an implicit approach (Kemin, Yan, & Xianming, 1997; Kemin, Zhen, Yan, & Kezhi, 1997; Xu et al., 2001), meanwhile

six use an explicit approach (Jalali Aghchai, Razani, & Mollaei Dariani, 2012a; Lexian & Dariani, 2008; Li, Hao, Lu, & Xue, 1998; Mohebbi & Akbarzadeh, 2010; Parsa, Pazooki, & Nili Ahmadabadi, 2008; Wong, Lin, & Dean, 2005). Wong, Dean, and Lin (2004) compare both approaches. Only two papers (Li et al., 1998; Xu et al., 2001) model numerically the friction between roller and workpiece, (while other authors neglect friction contributes to displacement). Most use commercial software (e.g. ABAQUS) which has been modified to incorporate appropriate solution codes (Marini et al., 2016).

Investigations into flow forming are frequently connected to the manufacture of near-net-shape parts that are finished using traditional machining. The avoidance, or at least the minimization, of machining and raw materials can be delivered by the adoption of flow forming of technology but only if applied to appropriate components. Thus a flow forming feasibility assessment methodology is critical to allow evaluation of how easy, or difficult, it is to produce a component with this cold forming technology. Steps of the feasibility assessment methodology are:

- (1) Find potential products where flow forming could be used.
- (2) Design a nominal flow forming process (e.g. specify a sequence of reduction ratios) for the candidate components.
- (3) Establish the feasibility (technological, qualitative and economic) for the production of the components, selected in step 1, by considering:
 - (a) Technological feasibility: verifying if it is possible to realize a specific component using current flow forming technology.
 - (b) Quantitative feasibility: analyzing theoretically the final properties of flow formed product.
 - (c) Economic feasibility: evaluate the cost and lead-time of flow forming designed processes.
- (4) Explore variations on the nominal process plan generated in Step 2 to identify the one that is most likely to produce the required quality of product.

2. Flow forming feasibility methodology

The proposed flow forming methodology is composed of three main parts (Figure 2) that can be characterized as: Product selection, Process analysis and Comparative analysis. The product selection step identifies potential products from a large number of candidate components (catalogs or assemblies), using high level criteria. This permitted a selection of

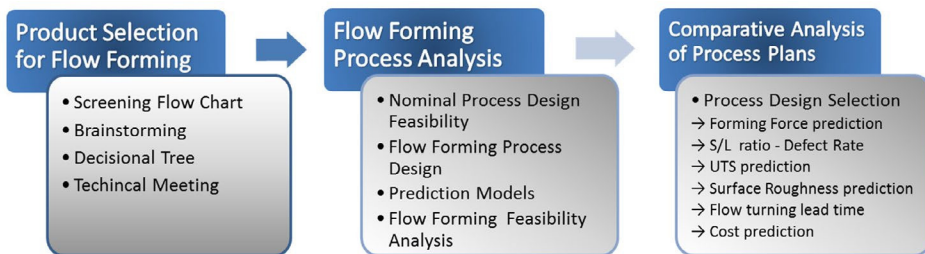


Figure 2. Flow forming feasibility methodology.

components in which the flow forming manufacturing process could result in added value in term of, say, quality enhancement and/or savings.

The manufacturability analysis requires both component dimensions and a process design. For the components that reach the final step of the feasibility assessment number of different potential flow forming process plans are developed for every part, in order to evaluate alternative forming strategies. A geometric representation of each component is used to provide the dimensions needed to allow selection of the most appropriate process plan. The quality targets incorporated in the system described here are the final material strength and the surface finish. Manufacturing cost and time have been developed via an industrial case study that provides information for a hybrid cost model. This suggested it was credible to estimate process costs, by relating them to analytical estimates of forming power and machine idle time.

A comparative analysis selects the best flow forming process designs in terms of feasibility and impact on quality and costs. Process design selection was made by comparison between forming forces and technological constrains. The forming forces and defect rate are used as evaluation parameters that determine the technological feasibility. During the process design selection phase, the final products' ultimate strength and surface roughness can be compared with target performance values between the designed flow forming alternatives. Similarly, flow forming costs and lead-times can be evaluated, also comparing them with real process parameters. At this stage, it is possible to detect best possible flow forming solution, depending on the target requirements. The following sections now describe each step shown in Figure 2 in more detail.

2.1. Product selection procedure

Product selection procedure is based on four stages (Figure 3)

- (5) Initial screening flow chart (Figure 4): enables high level filtering of components to identify potential candidates for further investigation.
- (6) Brainstorming: reduces further forming candidates and includes unconsidered components.
- (7) Decisional Tree (Figure 5): synthesis of acquired knowledge through critical flow forming application features identification.
- (8) Technical Meeting: discussion with production facilities or process expert about previous decisions (i.e. decisional tree developments).

Both the flow chart (Figure 4) and the decisional tree (Figure 5) have been developed from consideration of literature and industrial applications. The flowchart assess the main geometric constrains for flow forming applications (e.g. hollow circular axial symmetry and length and diameter ratio) while taking into account near net shape considerations (low



Figure 3. Product selection for flow forming methodology.

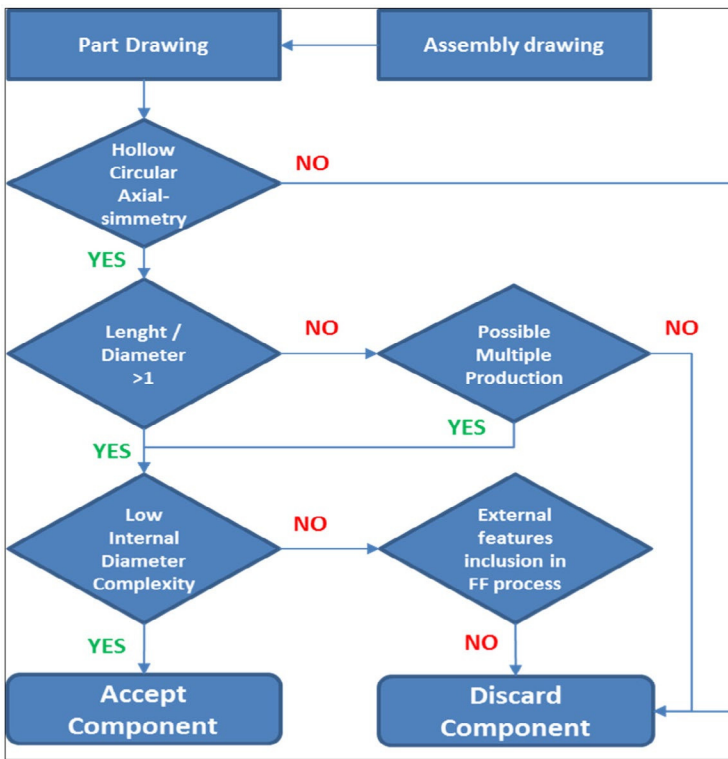


Figure 4. Product selection procedure chart.

internal complexity). Stacked production (i.e. the formation of several components from one preform) has been considered as alternative for uneconomic batches of one.

The decisional tree (Figure 5) investigates the following features:

- Material selection: material adequate to severe cold plastic deformation and its possible re-definition.
- Technological and Geometrical feasibility: possibility of realizing components geometry or semi-finished piece (propaedeutic to final geometry through further operations).
- Initial re-design Flow Forming oriented: possibility of final product design (or semi-finished design) in order to apply flow forming. These would include a series of rules that could be included in a Design for Flow Forming application. In Figure 5, some of these logic possible rules were described.
- Enhancing critical to Qualities Product proprieties: previous evaluation of flow forming impact on the product quality features, in comparison with current production (e.g. ultimate strength enhancing due to hardening).
- Economic re-design or material selection: possibility of adapting flow forming impact in an economic advantage (e.g. possibility of reducing thickness or using cheapest less resistant material, due to hardening).
- Raw material saving: dependent on current process. Flow forming could be an improvement if compared with pure machining or die forging processes. On the other hand, die casting and mold casting made an almost complete material usage.

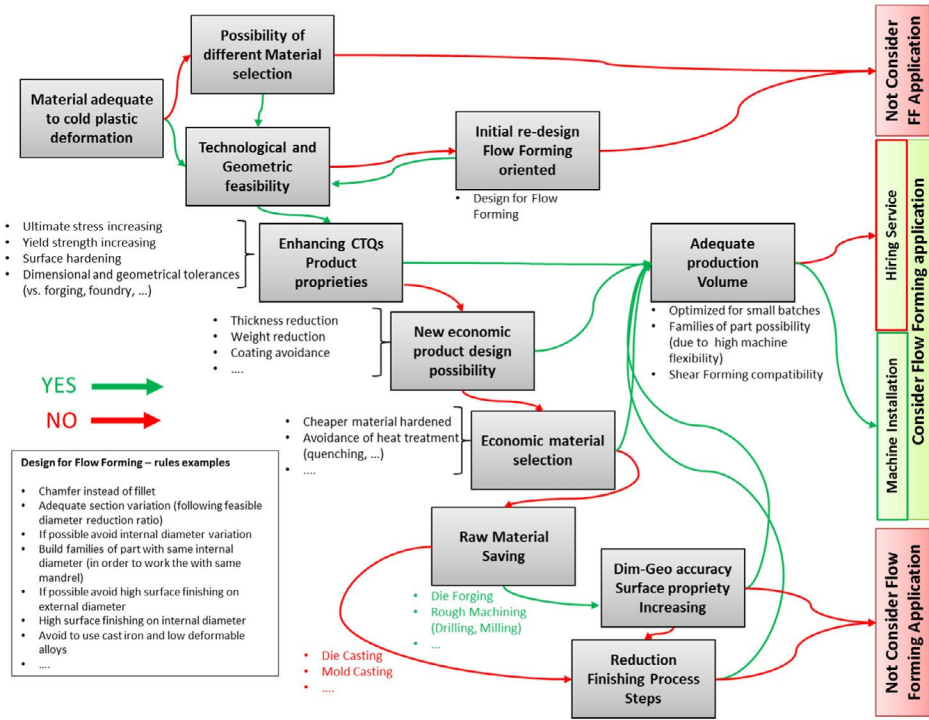


Figure 5. Decisional tree for flow forming product selection.

- Dimensional-Geometrical accuracy and Surface propriety increasing: flow forming’s ranges of tolerances and surface quality needed a comparison with the current process.
- Reduction Finishing Process Steps: evaluating the impact of flow forming on the process chain, through its semi-finished product characteristics.
- Production Volume: flow forming production is optimized for small batches, but enough for amortizing operational costs. Making family of part was considered a huge opportunity, particularly related with shear forming process compatibility.

Machine flexibility is often not enough, in order to justify high flow forming machine costing. So, service hiring was depicted as a concrete opportunity. This stage made an important impact not only on the product selection, but it gave also hints on product and process design development.

2.2. Process analysis

Process analysis has been defined by four phases (Figure 6): product design, flow forming process design, prediction models and flow forming feasibility.

2.2.1. Nominal process design feasibility

In this phase, the final component’s geometry and material selection are considered. The first is fundamental for designing the forming steps, while the latter has an enormous influence on the overall process definition (i.e. process parameters and intermediate forming steps).

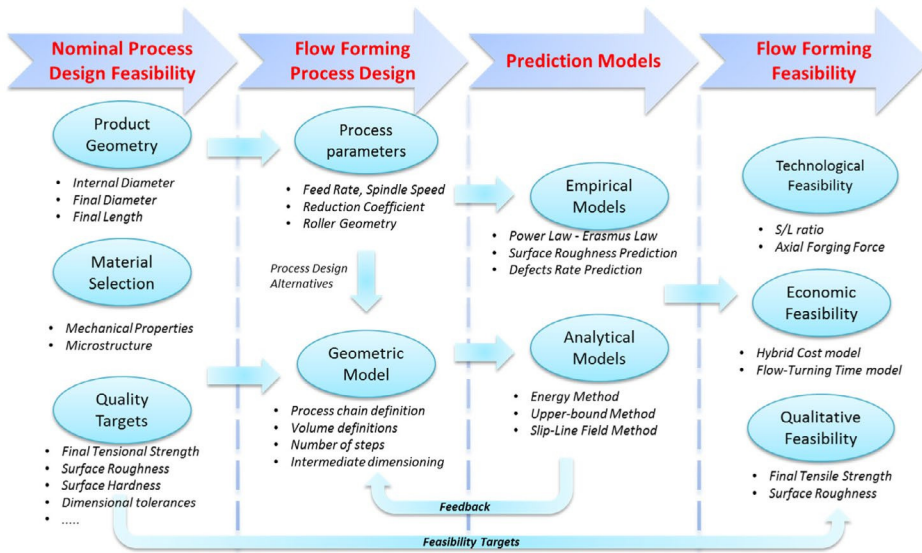


Figure 6. Flow forming process analysis chart.

2.2.1.1. Product geometry. Initial input data are the final geometry of the product (listed as follows), which are the data who lead the process design.

- Final diameter
- Final length
- Final piece features (flange diameters, flange lengths, internal walls thickness, chamfer degree, ...)
- Internal diameter (constant)

Internal diameter remained constant for whole process because it was constrained by mandrel. Reduction ratios selection depends on number of forming steps and its selection influences dimensioning of forming parts. In order to apply flow forming process, some modifications were needed in product drawing. For example on a tube, drastic section changes (vertical scale or high degree chamfers) or fillets must not be formed so chamfers with low degree should replace them instead. If first geometry was needed, this should be obtained by further machining operations.

2.2.1.2. Material selection. The sensitivity of the flow forming process to material properties affects the prediction accuracy and, so the impact, of theoretical models (Marini et al., 2016). This As stated in all literature and summarized by (Wong, Dean, & Lin, 2003) and (Sivanandini, Dhama, & Pabla, 2012), flow forming process was able to work on a huge range of material. An incomplete list of workable material has been deployed as follows: Aluminum alloys, Titanium alloys, Carbon steels, Low- and High-Alloy steels, Nickel alloys, Maraging steels, Inconel, Duplex, Copper, Brass. Eventual material changes should be defined at this stage. Reason for different new material selection would be caused by several reasons: incompatibility with severe; cold plastic deformation (e.g. cast iron); economic material selection; mechanical proprieties material increasing (due to their

increasing provided by forming hardening); quality target definition (e.g. dimensional tolerances, surface roughness); avoidance of welding or other operations through flow forming application. In particular, hardening provided by cold deformation could permit to select a less strong material in order to improve its mechanical properties. Another possibility could be to keep same material but reducing dimension. These possibilities would be limited by other factors of dimensioning such as corrosion. A complete knowledge about product loads and tensional state was needed in order to correctly approach these changes.

Quality targets definition was contemporary deployed with product design and material selection. Targets were defined by stakeholder needs and improvement possibilities, for example:

- Ultimate tensile strength
- Yield strength
- Surface Roughness
- Surface Hardness
- Dimensional tolerances
- Geometric tolerance (concentricity, ovality, cylindricity ...)
- Defects absence (wrinkling, circumferential cracks, radial cracks ...)

The failure prediction models and the dependency between quality target and failure is summarized in (Marini et al., 2016) and (Marini et al., 2015). Table 1 summarizes some of them. In this case, the quality targets that that can be measured through analytical models are used in the final comparison (ultimate tensile strength, surface roughness and defect prediction), whilst other can be used as process selection justification (i.e. to test in the experimental or numerical phase).

2.2.2. Flow forming process design

Different processes are developed for every component, in order to evaluate different forming strategies. Process parameters and reduction ratios (i.e. diameter reduction for every forming step) first selections have been based on literature and industrial examples. A geometric modeling method (i.e. using volume constancy) is used to select suitable intermediate dimension for every designed reduction step in a multistage flow forming process. In a first approximation, more than one process chain should be developed, in order to increase the feasibility to many combination of flow forming steps, process parameters and process design combinations.

2.2.2.1. Process parameters selection. The following process parameters need to be selected for designing a flow forming process:

- Number of steps: usually from 1–3. This selection is critical for the process parameters configuration.
- Reduction ratio: Ratio between the diameter of the hollow tube before the flow forming and the one after, defined in as $t = \left(\frac{D_i}{D_0}\right)$ (4). Selection of this parameter is dependent to number of steps. In case of more than one step, total reduction coefficient needed to respect needed final deformation. Reduction ratio is most important parameter in flow forming and its selection critical, as stated by (Hayama & Kudo, 1979b) and proved by several authors. Reduction ratios were selected from literature for similar


Table 1. Influences of process parameters on defects and geometrical inaccuracies (H, high; L, low; n/a, not available; n/c not clear) (Marini et al., 2015).

Defects types	Possible influences										
	Feed rate	Mandrel speed	Depth of cut	Reduction Ratio	Preform initial thickness	Roller Dimension	Roller attack angle	Preform microstructure	Preform Hardness	Lubricant	Heat treatments
Diametral growth	Hi	Lo	n/c	Hi	Lo	Hi	Hi	Lo	Lo	n/a	Lo
Ovality	Hi	Lo	Hi	Hi	n/c	Hi	n/c	Hi	Hi	n/a	Lo
Fish Scaling	Hi	Lo	Lo	Hi	Hi	n/c	Hi	Hi	n/a	n/a	Hi
Wrinkling	Hi	Lo	n/a	Hi	Hi	n/c	Hi	n/a	n/a	n/c	Hi
Springback	Hi	n/a	n/a	Hi	Hi	Hi	n/a	Hi	Hi	n/a	Hi
Cracking	Hi	Lo	Hi	Hi	Hi	n/c	Hi	Hi	n/c	n/c	Hi
Microcrackings	n/c	n/a	n/a	n/c	n/c	n/a	n/a	Hi	n/c	n/a	n/c

material and adapted to current dimensions, (Roy, Klassen, & Wood, 2009), (Singhal et al., 1987) and (Chang et al., 1998).

- Roller geometry: attack angle (α) and roller diameter (DR). Roller geometry was selected in order to have less force impact and low defects rate. Also these parameters were taken from literature (Hayama & Kudo, 1979a; Jahazi & Ebrahimi, 2000; Srinivasulu, Komaraiah, & Rao, 2012a) in dependence to selected reduction ratios and passes number.
- Spindle speed and feed rate can be deducted from literature or industrial application, due to the previous parameters selection. In particular, feed rate had strict connection with roller attack angle and reduction ratios, as summarized in (Music, Allwood, & Kawai, 2010), (Marini et al., 2016) and (Wong et al., 2003). Feed rate impacted on axial forces, surface roughness, defects and process cost. Articles such as Jalali Aghchai et al. (2012), Davidson et al. (2008) Srinivasulu et al. (2012b) and Davidson et al. (2008) can be used to evaluate usable parameters settings.

The selection of process parameters is always an iterative process. This selection is not optimized but a first draft, which can be still considered reliable for judging the process feasibility. This happens because of process parameters range and their connection with geometries and materials (Marini et al., 2015).

2.2.2.2. Geometric model. Product geometry should be assigned to every forming pass. Using reduction ratios, it is possible to deduct all semi-finished components geometries. Initial blank (preform) is usually dimensioned as a hollow cylinder (Podder et al., 2012; Rajan, Deshpande, & Narasimhan, 2002a). Volume constancy is widely used in literature for evaluating flow forming blank and preform dimensions (Podder et al., 2012; Singhal et al., 1987). Same methodology can be used for dimensioning the intermediate forging geometries during the flow forming steps.

In Appendix 1, the mathematical expression volume constancy and its derivation of for deriving the initial and intermediate geometries is displayed (4–8). Results of this mathematical expression (8) are numbers with high number of decimal precision (four decimals), for preform and intermediates. This required a high level measurement for being prepared, also for a low precision in input data (one decimal). Final dimensions need different tolerances. These tolerances were selected for rounding final length and testing selected parameters through inverse evaluation of preform diameter. So a procedure has been set in order to evaluate blank dimensions and reduction ratios selections, having tolerances selected. Figure 7 showed developed procedure. Rounding down initial length L'_0 to selected number of digits (one, two or four decimals), it was possible to obtain another L_0 value. With the latter, it was possible to evaluate the internal diameter D_1 through the inverse volume constancy expression (8). After, it was possible to accept or reject blank or preform dimensions, if obtained D_0 resulted to agree with tolerances. In case of not agreement, initial blank or preform dimensions and reduction ratios needed to be changed. The procedure can be replicated at the same for multi-pass processes, as exposed in Figure 8. Expression (8) is valid only for passing from a cylindrical tube to another. This relationship needed to be modified, in order to describe more complicated shape, shape, as in Equations (11–14). Given the precision and the opportunity of producing complex shapes, volume constancy can be modified for obtaining complex shape. In Appendix 2, volume constancy has been

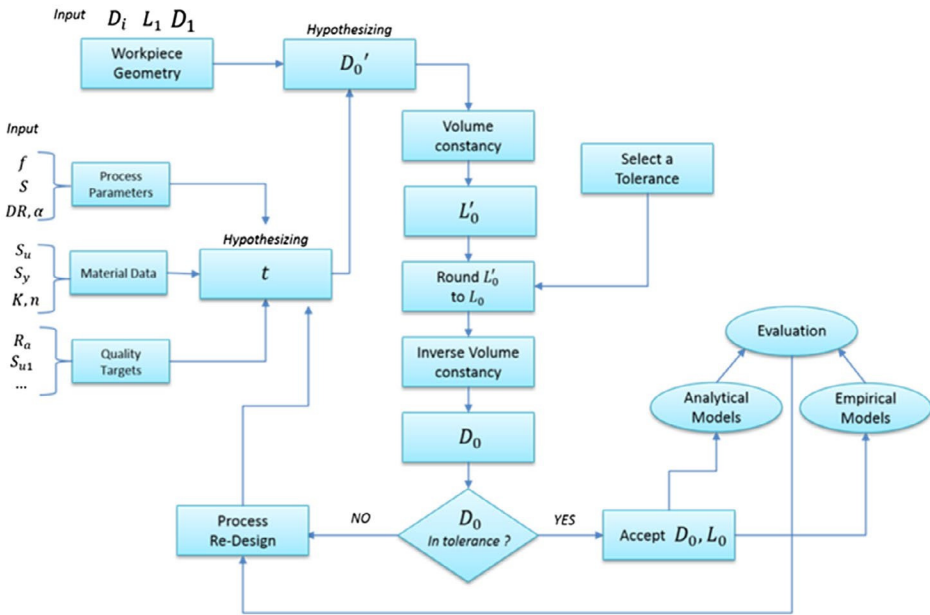


Figure 7. Geometric modeling flowchart for single multi stage flow forming.

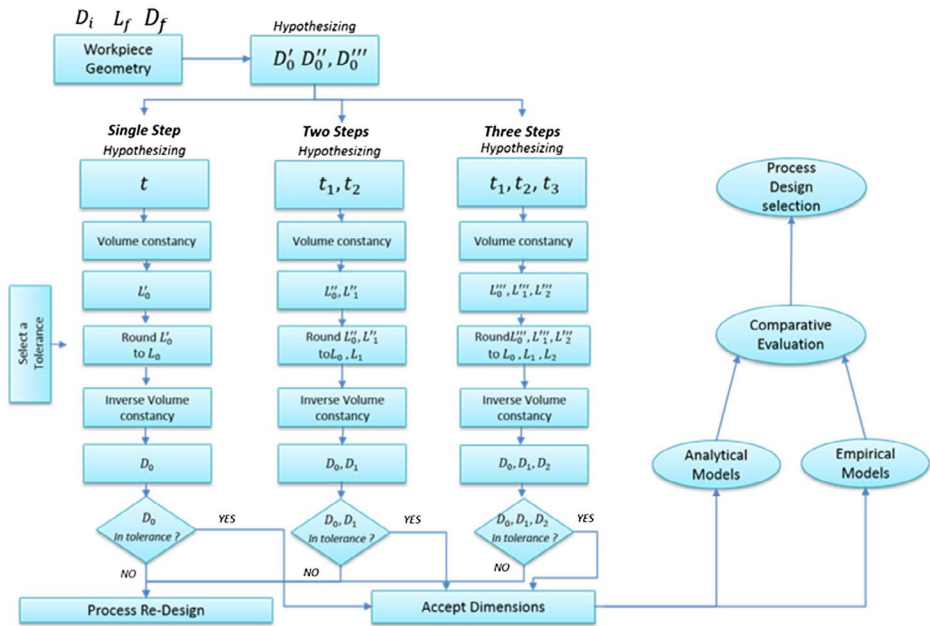


Figure 8. Geometric modeling flowchart for multi stage flow forming.

modified for equalizing a tubular blank volume with a flanged pipe one (i.e. this will be used in the case study). New features of flanged pipe were described as follows. In case of

very complex output or intermediate geometries, CAD and FEM supports are essential for dimension correctly the preform and intermediate shapes.

2.2.3. Prediction models

Using empirical models, the defect rate (equations (15–16)), ultimate tensile strength (equations (1, 2)) and surface finish, (equation (3)) can be deduced. The quality targets considered are the final material strength and surface finish.

2.2.3.1. Empirical models. Key to this process is the *S/L* ratio, developed Gur and Tirosh (1982) and validated by several authors (Jahazi & Ebrahimi, 2000; Jalali Aghchai, Razani, & Mollaei Dariani, 2012b; Parsa et al., 2008; Podder et al., 2012; Rajan & Narasimhan, 2001; Roy et al., 2010), expresses plastic flow quality for given process parameters. If axial contact length (*L*) exceeds the circumferential length (*S*), circumferential plastic flow dominates (*S/L* < 1) and geometrical inaccuracies and defects are common. Increasing the *S/L* ratio results in greater interfacial friction that enhances axial flow. In this case (*S/L* > 1), and most of material flows in axial direction consequently defects tend are infrequent. Although, if contact ratio becomes too large (*S/L* >> 1), friction coefficient become close to unity and material flows in directions smaller than the attack angle. In this case, wave-like surfaces and thickness variation in workpiece occur (Marini et al., 2015). Appendix 3 provides mathematical formulation of the *S/L* ratio.

Hollomon’s power law (1) is deployed by some authors (Jalali Aghchai et al., 2012b; Podder et al., 2012) for predicting the ultimate strength of formed components and shows good agreement with experimental data.

$$S_u = K \epsilon_u^n \tag{1}$$

With: *S_u*, ultimate tensile strength (MPa); *ε_u*, total plastic strain; *n*, strain hardening exponent; *K*, strength index (MPa).

Erasmus law (2), used in Rajan et al. (2002a), is derived from Hollomon’s one. This formula considers section variation (*A_r*) and accuracy in its prediction is tested by the authors

$$S_u = K \left[n + \ln \left(\frac{1}{1 - A_r} \right) \right]^n \tag{2}$$

where: $A_r = \frac{A_i - A_f}{A_i}$ is the area reduction ratio.

(Rajan & Narasimhan, 2001) develop an empirical formula (3) for flow forming, evaluating the surface finishing.

$$h = DR - \frac{1}{2} \sqrt{4DR^2 - f^2} \tag{3}$$

where, *h*, is height variations on the surface (mm); *DR*, is roller diameter (mm) and *f* is feed rate (mm/rev).

2.2.3.2. Analytical models. Using such analytical models, working forces and powers can be deduced, using component and roller geometries, materials and process parameters. Three main models have been proposed in the literature: energy model (Hayama & Kudo, 1979a, 1979b; Jolly & Bedi, 2010; Mohan & Misra, 1970; Molladavoudi & Djavanroodi, 2010;

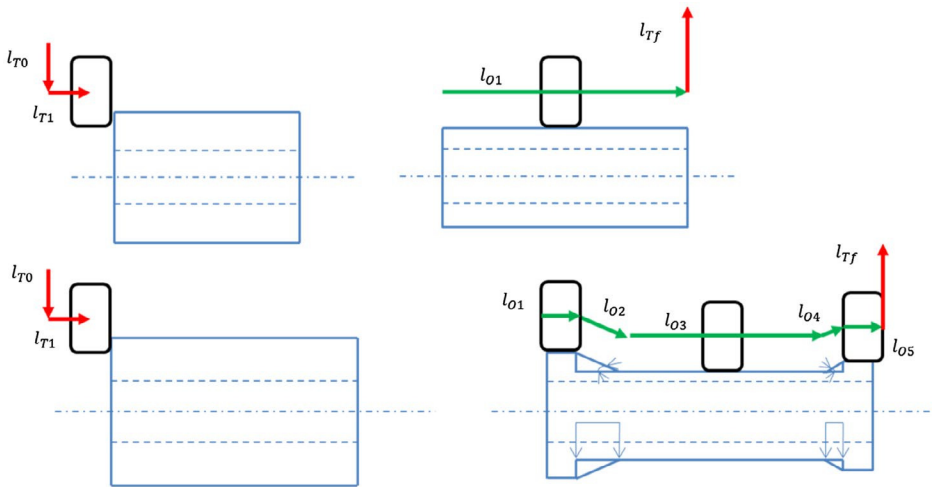


Figure 9. Flow forming time model schematization for hollow tube (up) and flanged pipe (down).



Figure 10. Flow forming feasibility analysis flowchart.

Singhal et al., 1990), upper-bound method (Gur & Tirosh, 1982; Park et al., 1997; Roy et al., 2009) and slip-line field (Nagarajan et al., 1981). Energy is the most frequently and complete applied and developed by researchers. In Appendix 2, principle forming forces and powers formula from (Hayama & Kudo, 1979a) have been developed for application. This phase provide also feedback to the process parameters and the intermediate process steps. Different combination of process should be needed for obtaining a suitable flow forming sequence.

2.2.4. Flow forming feasibility analysis

Figure 10 summarizes the feasibility analysis procedure. Technological feasibility should be assessed before proceeding with further steps (i.e. qualitative and economic).

Technological feasibility is determined by the axial forming force values (25) and the S/L ratios (15–16) for every process variant. First needs to be compared with industrial available flow forming machine, the second with a threshold value. The complete plastic deformation model can be found in Appendix 4.

Qualitative feasibility is determined by the comparison ultimate tensile strength (2) and surface roughness predictions (3) with current (or target) values.

2.2.4.1. Economic feasibility. A process time model has been developed by assuming the forming tool motion exhibits similarity between flow forming and turning processes. Model and its derivation are presented in Appendix 5. Time model has been constructed in reference to flow forming process dynamic. For this reason, a time-model is inspired by

classic G-code, which is used for programming CNC machines. Roller motion during flow forming process is schematized in Figure 9. Process time is obtained by the developed model, meanwhile the idle times and indirect costs have been estimated based on industrial case studies. As shown in Figure 9, forming lengths (green) and transverse lengths (red) can be treated differently as in turning. Consequently, forming lengths are associated to process feed rate. As shown in Equation (34), the process time can be calculated referring to the selected process parameters. A hybrid cost model has been used for calculating the total process costs (31), the complete cost model can be found in Appendix 5. Model is derived from cost models used in (Kalpakjian & Schmid, 2009; Swift & Booker, 2013). Forming powers (i.e. analytically calculated in the previous phase) have been used for calculating energy expenditures during the flow forming process (36). The obtained values of cost and time need to be compared with the current or the targets ones.

2.3. Comparative analysis of process plans

Depending on the quality target, the designed flow forming process alternatives, which have been defined as feasible, can be compared for defining the target optimal solution. Although, flow forming designs must be filtered for the defined technological feasibility (i.e. the upper limit of forming forces and the S/L threshold) and after evaluate qualitative (S/L threshold, UTS increasing threshold, surface roughness acceptable limit) and economic feasibilities (Figure 10). A weighted average of these different parameters can be realized, for summarizing the comparison between different flow forming process plans (i.e. sequences of reduction operations). Weights selection depends on the required quality and cost/time targets.

3. Case studies

Products from Weir Group PLC have been used for investigating the flow forming feasibility. Product selection has been applied on assemblies and catalogs. Due to disclosure agreement with the company, no details about the components (i.e. dimensions, tolerances, materials, mechanical proprieties, costs or lead times) or about the comparative analysis (i.e. quality or cost targets) can be revealed. Selected process variant for both the components is forward flow forming, due to high process stability and control of formed shape (Hayama & Kudo, 1979b). Integrals were solved numerically using Maple, in order to evaluate all energy contributions. After filtering with the flow chart (Figure 3), 27 components were selected. Brainstorming reduces them to 5, mainly due to the repetition of certain components in the assemblies. Decisional tree reduced them to 2: a riser pipe and valve seat. For the latter, stacked production has been considered as forming option. In comparison with the current manufacturing process, strength improvement, dimensional tolerances close to the final shape and less machining (i.e. even if the stacked component need to be thermal treated before being separated) can be improved through flow forming process, even if the material and its resilience put the process on the borderline of unfeasibility.

Riser pipe is very long and is essentially a flanged pipe (so the main potential advantage of production by flow forming would be removal of the need for welding of the flange).

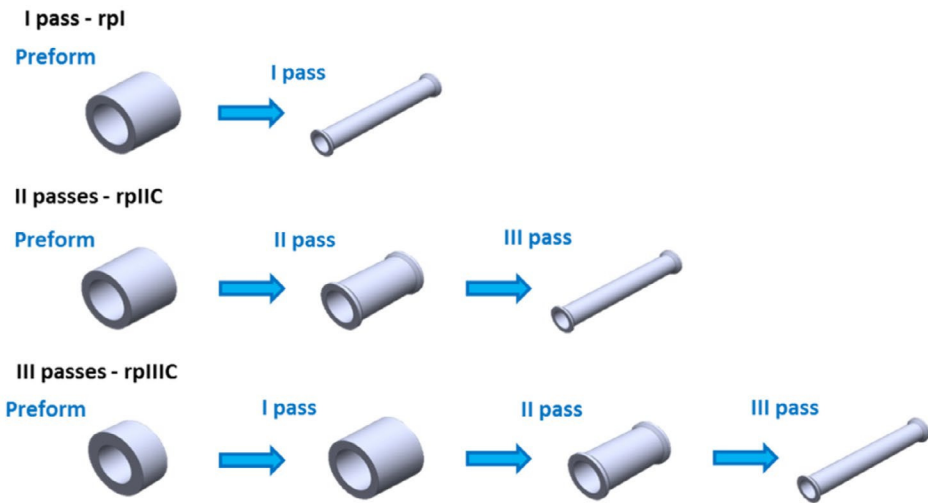


Figure 11. Some of the designed flow forming processes for seat valve manufacturing: rpl (top), rplIC (middle), rplIIC (bottom).

3.1. Nominal process feasibility

Riser pipe is modeled as in Figure 11. Diametric steps were substituted by chamfers of different degrees. Differences between diameters allowed trying different chamfer solution (30 and 40 degrees angles). Presence of slot in planar face and drilled holes must be machined after forming process. Flanges diameters were defined as same of initial product but formed with different options. Piece geometry needed to be changed (chamfer in diametrical steps). These changes were considered compatible with component usage, also if more material needed to be removed by drilling. Material has been selected by prior design, due to compatibility with corrosive environment and loads. Material was a steel with following characteristics: yield strength, 820 MPa; ultimate Tensile strength, 850 MPa; hardening exponent (n), 0.25; strength index (K), 820 MPa.

3.2. Flow forming process design

Reduction ratios (4) have been iterative selected using the procedures in Figure 7, for single pass, and in Figure 8, for multiple passes (0.1 mm. tolerance). Reduction ratios' ranges were taken from literature (Roy et al. (2009)) even if only dedicated experimental and numeric analysis should correctly evaluate feasible reduction ratios. This was due to high flow forming process instability (Hayama & Kudo, 1979a). Many process alternatives were created (i.e. forming in one, two or three steps and creating the flanges in different steps), described in Table 2. Different forming strategies have been created for producing the component:

- Type A: hollow cylinder blank is formed into flanged pipe only in the last stage, including chamfers of 30° (remaining a regular pipe for one or two stages).
- Type B: hollow blank is formed flanged pipe (at second stage for three passes) with chamfers of 30°. In the last stage, main diameter is only processed, without involving flanges.

- Type C: hollow blank (for two stages) or pipe (three stages) is formed as flanged pipe (30° chamfers). In the last stage, pipe are formed as flange one with 45° degrees chamfers (Figure 11).
- Type D (only for three stages): all stages were formed as flange pipe including chamfers and flanges variations. Hollow blank is formed with 20° chamfers, first pass with 30° and third pass with 45°.

Reduction ratios and process variants are summarized in Table 2. Process parameters were selected accordingly to literature (Hayama & Kudo, 1979a; Podder et al., 2012; Rajan & Narasimhan, 2001; Srinivasulu, Komaraiah, & Rao, 2012b): spindle speed, 300 rpm; feed rate, 540 mm/min (1.8 mm/rev); mandrel diameter, 83 mm. Roller geometry were selected accordingly to (Hayama & Kudo, 1979b) and (Jahazi & Ebrahimi, 2000): roller diameter, 800 mm; roller attack angle, 20°.

3.3. Prediction models

Forming axial forces, defect rate prediction (S/L) and final predicted proprieties (i.e. ultimate tensile strength and surface roughness) have been summarized as in Table 3. In two passes processes, last stages involved a huge material displacement amount, due to high thickness differences and process parameters. In three stages, trend became normal because of force decreasing. This was due to material displacement divided though more forming operations. S/L ratio trends correctly assume values coherent with forming forces, except that in two cases (second passes type A and type C processes).

3.4. Flow forming feasibility

Axial forming force limit has been established 10,000 KN (AFRC machine limit), defect rate threshold, $S/L > 1$ (as in (Gur & Tirosh, 1982)), and strength increasing ratio threshold, 0.25 (arbitrary selected). Referring to Table 3, the unfeasible features were target in red, meanwhile feasible parameters in green. Technological feasibility is found only acceptable for four cases (i.e. mostly due to the high forces involved), although even then the likely defect rate was very high. In conclusion only one process has been selected as feasible the process might enhance the tensile strength and surface roughness and reduce lead times the cost increase resulted in the conclusion the process was not a feasible proposition for the component. Following these criteria, only process rpIIIB has been considered as feasible.

Qualitative feasibility is evaluated through the ultimate strength increasing (i.e. which follows the reduction ratios trend). Surface roughness was not coherent with industrial and literature data (Wong et al., 2003). Strength improvement, even if significant, was not a primary target, due to the low loads on the component and its unknown impact on the current erosion-corrosion phenomenon on the riser pipe. Economic feasibility has evaluated only for the selected process. Flow forming times and costs data have been taken from industrial case study and machine available at Advanced Forming Research Center (AFRC) in Glasgow. Final process time shows a reduction of 60% with the current production time, although predicted cost result 25% higher than the current one. Even though the process results technologically feasible and the prediction models show possible improvements in

Table 2. Process variants description, number of stages (passes), reduction ratios and trends.



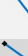









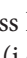

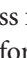
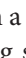
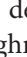
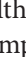
Process code	Passes nr.	Description				Redution Ratios			Total Reductio	Thickness Trend	Valves created
		Blank	Pass I	Pass II	Pass III	Pass I	Pass II	Pass III			
svI4	1	Pipe	Multiple flanged tube			0.18			0.18		4
svII4	2	Pipe	Pipe	Multiple flanged tube		0.23	0.12		0.32		4
svII6	2	Pipe	Pipe	Multiple flanged tube		0.25	0.18		0.34		6
svIII6	3	Pipe	Pipe	Pipe	Multiple flanged tube	0.14	0.13	0.12	0.34		6
svIII8	3	Pipe	Pipe	Pipe	Multiple flanged tube	0.18	0.16	0.09	0.37		8
svIII16	3	Pipe	Pipe	Pipe	Multiple flanged tube	0.2	0.16	0.12	0.41		16

Table 3. Prediction model results: axial forming forces and trend, ultimate tensile strengths and increments, surface roughness, S/L ratios and trends.

Process code	Axial Forming Force (KN)			Axial F Trend	Ultimate Strenght		Predicted Surface Roughness (μm)	S/L ratio			S/L ratio Trend
	Pass I	Pass II	Pass III		Predicted UTS (Mpa)	Increment		Pass I	Pass II	Pass III	
svI4	764.36				1288.08	615.31	70.31	0.982			
svII4	896.27	148.89			1432.12	684.22	70.31	0.708	1.519		
svII6	932.28	491.31			1456.98	696.12	70.31	0.632	1.519		
svIII6	430.92	388.12	389.14		1447.75	691.70	70.31	1.173	1.351	1.519	
svIII8	1652.03	287.09	411.79		1475.17	704.82	70.31	0.856	1.080	2.090	
svIII16	1683.23	811.89	92.28		1498.57	716.02	70.31	0.990	1.437	1.996	

strength and lead time, the process has been considered as unfeasible for this component due the predicted cost increasing (i.e. very high cost impact on the comparative analysis).

Similarly a flow forming process for a valve seat was designed to be produced in a stack (i.e. 4, 6 or 8 from the same preform) with a proportional increasing of forming steps. Technologically, the process was deemed acceptable for many combinations. Although ultimate strength and surface roughness have been considered as acceptable (i.e. compared with previous manufacturing method) as well as the lead time (i.e. almost halved), the cost has doubled in comparison with the current cost (based on forging and machining).

4. Conclusion

This methodology provides a reliable guidance for finding opportunities an evaluating the feasibility of flow forming process. Although the analytical model can formulate the process in a complete way, they are not sufficient for analyzing completely the flow forming process. Process parameters and design selection should interact directly with the feasibility study, giving an immediate feedback and not acting as hypothesis. A more complete framework should be developed in this sense, including numerical capabilities and approaches.

Acknowledgements

The authors want to thank WARC (Weir Advanced Research Center), Weir Group PLC, Advanced Forming Research Center (AFRC) and DMEM (Department of Design, Manufacturing and Engineering Management) of the Strathclyde University of Glasgow for the fundamental and continuous support in this research.

Disclosure statement

No potential conflict of interest was reported by the authors.

Funding

This research is a part of Research Chair in Advanced Forming and Forging project (EPSRC funding: EP/H03465X/1), conducted by the University of Strathclyde (DMEM) and several partners.

ORCID

Daniele Marini  <http://orcid.org/0000-0003-3672-6017>

References

- Allen, A. J., & Swift, K. G. (1990). Manufacturing process selection and costing. *Proceedings of the Institution of Mechanical Engineers, Part B: Journal of Engineering Manufacture*, 204, 143–148. doi:10.1243/PIME_PROC_1990_204_057_02
- Chang, S.-C., Huang, C., Yu, S.-Y., Chang, Y., Han, W.-C., Shieh, T.-S., ... Wang, W.-S. (1998). Tube spinnability of AA 2024 and 7075 aluminum alloys. *Journal of Materials Processing Technology*, 80–81, 676–682. doi:10.1016/S0924-0136(98)00174-5
- Davidson, M. J., Balasubramanian, K., & Tagore, G. R. N. (2008). Experimental investigation on flow-forming of AA6061 alloy – A Taguchi approach. *Journal of Materials Processing Technology*, 200, 283–287. doi:10.1016/j.jmatprotec.2007.09.026
- Gupta, R. K., Ghosh, B. R., Kumar, V. A., Karthikeyan, M. K., & Sinha, P. P. (2007). Investigation of cracks generated during flow forming of Nb–Hf–Ti alloy sheet. *Journal of Failure Analysis and Prevention*, 7, 424–428. doi:10.1007/s11668-007-9089-2
- Gur, M., & Tirosh, J. (1982). Plastic flow instability under compressive loading during shear spinning process. *Journal of Engineering for Industry*, 104, 17–22.
- Hayama, M., & Kudo, H. (1979a). Analysis of diametral growth and working forces in tube spinning. *Bulletin of JSME*, 22, 776–784.
- Hayama, M., & Kudo, H. (1979b). Experimental study of tube spinning. *Bulletin of JSME*, 22, 769–775.
- Jahazi, M., & Ebrahimi, G. (2000). The influence of flow-forming parameters and microstructure on the quality of a D6ac steel. *Journal of Materials Processing Technology*, 103, 362–366.
- Jalali Aghchai, A., Razani, N. A., & Mollaei Dariani, B. (2012). Flow forming optimization based on diametral growth using finite element method and response surface methodology. *Proceedings of the Institution of Mechanical Engineers, Part B: Journal of Engineering Manufacture*, 226, 2002–2012. doi:10.1177/0954405412461328
- Jolly, S. S., & Bedi, D. S. (2010). Analysis of power and forces in the making of long tubes in hard-to-work materials. *Proceedings of the World Congress on Engineering, II*.
- Kalpakjian, S., & Schmid, S. R. (2009). *Manufacturing engineering and technology* (6th ed.). Upper Saddle River, NJ: Prentice Hall. doi:0136081681.
- Kemin, X., Yan, L., & Xianming, Z. (1997). The disposal of key problems in the FEM analysis of tube stagger spinning. *Journal of Materials Processing Technology*, 69, 176–179. doi:10.1016/S0924-0136(97)00014-9

- Kemin, X., Zhen, W., Yan, L., & Kezhi, L. (1997). Elasto-plastic FEM analysis and experimental study of diametral growth in tube spinning. *Journal of Materials Processing Technology*, 69, 172–175. doi:10.1016/S0924-0136(97)00013-7
- Lexian, H., & Dariani, B. M. (2008). An analytical contact model for finite element analysis of tube spinning process. *Proceedings of the Institution of Mechanical Engineers, Part B: Journal of Engineering Manufacture*, 222, 1375–1385. doi:10.1243/09544054JEM1202
- Li, K., Hao, N., Lu, Y., & Xue, K. (1998). Research on the distribution of the displacement in backward tube spinning. *Journal of Materials Processing Technology*, 79, 185–188. doi:10.1016/S0924-0136(98)00009-0
- Marini, D., Cunningham, D., & Corney, J. R. (2015). A review of flow forming processes and mechanisms. *Key Engineering Materials*, 651–653, 750–758.
- Marini, D., Cunningham, D., Xirouchakis, P., & Corney, J. R. (2016). Flow forming: A review of research methodologies, prediction models and their applications. *International Journal of Mechanical Engineering & Technology*, 7, 285–315.
- Mohan, T. R., & Misra, R. (1970). Studies on power spinning of tubes. *International Journal of Production Research*, 10, 351–364.
- Mohebbi, M. S., & Akbarzadeh, A. (2010). Experimental study and FEM analysis of redundant strains in flow forming of tubes. *Journal of Materials Processing Technology*, 210, 389–395. doi:10.1016/j.jmatprotec.2009.09.028
- Molladavoudi, H. R., & Djavanroodi, F. (2010). Experimental study of thickness reduction effects on mechanical properties and spinning accuracy of aluminum 7075-O, during flow forming. *The International Journal of Advanced Manufacturing Technology*, 52, 949–957. doi:10.1007/s00170-010-2782-4
- Music, O., Allwood, J. M., & Kawai, K. (2010). A review of the mechanics of metal spinning. *Journal of Materials Processing Technology*, 210, 3–23. doi:10.1016/j.jmatprotec.2009.08.021
- Nagarajan, H. N., Kotrappa, H., Mallanna, C., & Venkatesh, V. C. (1981). Mechanics of flow forming. *CIRP Annals – Manufacturing Technology*, 30, 159–162. doi:10.1016/S0007-8506(07)60915-9
- Park, J.-W., Kim, Y.-H., & Bae, W.-B. (1997). Analysis of tube-spinning processes by the upper-bound stream-function method. *Journal of Materials Processing Technology*, 66, 195–203. doi:10.1016/S0924-0136(96)02519-8
- Parsa, M. H., Pazooki, A. M. A., & Nili Ahmadabadi, M. (2008). Flow-forming and flow formability simulation. *The International Journal of Advanced Manufacturing Technology*, 42, 463–473. doi:10.1007/s00170-008-1624-0
- Podder, B., Mondal, C., Ramesh Kumar, K., & Yadav, D. R. (2012). Effect of preform heat treatment on the flow formability and mechanical properties of AISI4340 steel. *Materials & Design*, 37, 174–181. doi:10.1016/j.matdes.2012.01.002
- Rajan, K. M., Deshpande, P. U., & Narasimhan, K. (2002a). Effect of heat treatment of preform on the mechanical properties of flow formed AISI 4130 – A theoretical and an experimental assessment. *Journal of Manufacturing Processing Technology*, 125–126, 503–511.
- Rajan, K. M., Deshpande, P. U., & Narasimhan, K. (2002b). Experimental studies on bursting pressure of thin-walled flow formed pressure vessels. *Journal of Materials Processing Technology*, 125–126(Citazione sotto), 228–234.
- Rajan, K. M., & Narasimhan, K. (2001). An investigation of the development of defects during flow forming of high strength thin wall steel tubes. *Practical Failure Analysis*, 1, 69–76.
- Roy, M. J., Klassen, R. J., & Wood, J. T. (2009). Evolution of plastic strain during a flow forming process. *Journal of Materials Processing Technology*, 209, 1018–1025. doi:10.1016/j.jmatprotec.2008.03.030
- Roy, M. J., Maijer, D. M., Klassen, R. J., Wood, J. T., & Schost, E. (2010). Analytical solution of the tooling/workpiece contact interface shape during a flow forming operation. *Journal of Materials Processing Technology*, 210, 1976–1985. doi:10.1016/j.jmatprotec.2010.07.011
- Singhal, R. P., Das, S. R., & Prakash, R. (1987). Some experimental observations in the shear spinning of long tubes. *Journal of Mechanical Working Technology*, 14, 149–157.
- Singhal, R. P., Saxena, P. K., & Prakash, R. (1990). Estimation of power in the shear spinning of long tubes in hard-to-work materials. *Journal of Materials*, 23, 29–40.

Sivanandini, M., Dhami, S. S., & Pabla, B. S. (2012). Flow forming of tubes-a review. *International Journal*, 3(5), 1–11.

Srinivasulu, M., Komaraiah, M., & Rao, C. (2012a). Experimental investigations to predict mean diameter of AA6082 tube in flow forming process – A DOE approach. *IOSR Journal of Engineering*, 2, 52–60. Retrieved from <http://www.academia.edu/download/30370249/H0265260.pdf>

Srinivasulu, M., Komaraiah, M., & Rao, C. S. K. P. (2012b). Experimental studies on the characteristics of AA6082 flow formed tubes. *Journal of Mechanical Engineering Research*, 4, 192–198. doi:10.5897/JMER11.063

Swift, K. G., & Booker, J. D. (2013). Manufacturing process selection handbook. *Manufacturing Process Selection Handbook*, 141–174. doi:10.1016/B978-0-08-099360-7.00005-7

Wong, C., Dean, T., & Lin, J. (2003). A review of spinning, shear forming and flow forming processes. *International Journal of Machine Tools and Manufacture*, 43, 1419–1435. doi:10.1016/S0890-6955(03)00172-X

Wong, C. C., Dean, T. A., & Lin, J. (2004). Incremental forming of solid cylindrical components using flow forming principles. *Journal of Materials Processing Technology*, 153–154, 60–66. doi:10.1016/j.jmatprotec.2004.04.102

Wong, C. C., Lin, J., & Dean, T. A. (2005). Effects of roller path and geometry on the flow forming of solid cylindrical components. *Journal of Materials Processing Technology*, 167, 344–353. doi:10.1016/j.jmatprotec.2005.05.039

Xu, Y., Zhang, S., Li, P., Yang, K., Shan, D., & Lu, Y. (2001). 3D rigid–plastic FEM numerical simulation on tube spinning. *Journal of Materials Processing Technology*, 113, 710–713. doi:10.1016/S0924-0136(01)00644-6

Appendix 1. Volume constancy

Reduction ratio t is defined as in (4)

$$t = \left(\frac{D_1}{D_0} \right) \tag{4}$$

Referring to Figure A1: D_0 , initial external diameter D_1 , final external diameter; D_p , internal diameter; L_1 , final length. Using volume constancy (5), we can obtain (6).

$$V_0 = V_1 \tag{5}$$

$$L_0 (D_0^2 - D_i^2) = L_1 (D_1^2 - D_i^2) \tag{6}$$

From (6), it is possible to obtain the final length L_1 (7).

$$L_0 = L_1 \left(\frac{D_0^2 - D_i^2}{D_1^2 - D_i^2} \right) \tag{7}$$

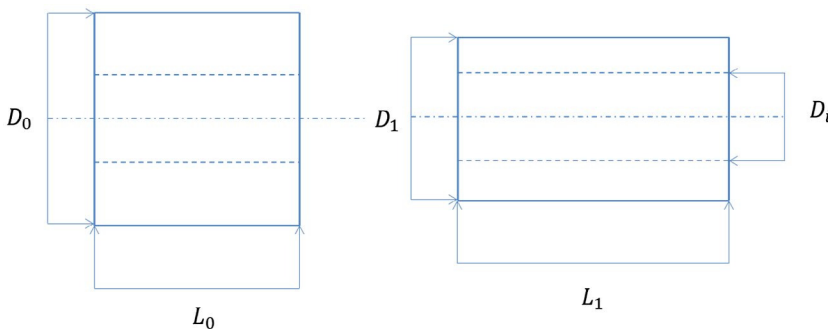


Figure A1. Decisional tree for flow forming product selection.

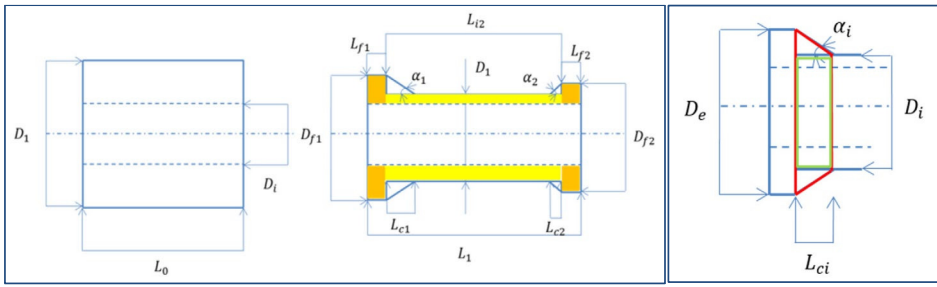


Figure A2. Volume constancy modification for a flanged pipe.

From (7), the initial diameter D_1 (7) is easily derivable.

$$D_0^2 = \sqrt{\frac{L_1(D_1^2 - D_i^2) + D_i^2}{L_0}} \quad (8)$$

Appendix 2. Volume constancy modification

Volume constancy (5) need to be modified for equalizing a tubular blank volume with a flanged component. Referring to Figure A2, the new features of flanged pipe are the flanges' lengths (L_{f1} , L_{f2}), flanges' diameters (D_{f1} , D_{f2}), chamfers' length (L_{c1} , L_{c2}) and chamfers' angles (α_1 , α_2). So, (5) could rewrite as (9).

$$V_1 = V_{f1} + V_{f2} + V_{i2} + V_{c1} + V_{c2} \quad (9)$$

Referring to Figure A2 (left), V_{f1} and V_{f2} correspond to flanges volume (orange), V_{c1} and V_{c2} to chamfer volume (white) and V_{i2} to internal volume (yellow). Flanges volume and internal volume could be calculated as cylindrical pipe. Chamfer volumes could be considered as hollow cone frustums. Referring to Figure A2, chamfer volume was calculate as in (10)

$$V_{ci} = \frac{1}{3} \pi L_{ci} \left(\frac{D_e^2 + D_e D_i + D_i^2}{4} \right) - \pi L_{ci} \frac{D_i^2}{4} \quad (10)$$

First member of equation represents the red zone in Figure A2 (right), and second member the green one. Defining the chamfer length $L_{ci} = \cot(\alpha_c) \frac{D_e - D_i}{2}$ and applying to (10):

$$V_{ci} = \frac{1}{24} \pi \cot(\alpha_c) (D_e^3 + 2D_i^3 - 3D_e D_i) \quad (11)$$

Using (11), modified volume constancy (9) could be written as follows.

$$\begin{aligned} L_1 (D_1^2 - D_i^2) &= L_{f1} (D_{f1}^2 - D_i^2) + L_{f2} (D_{f2}^2 - D_i^2) + L_2 (D_{i2}^2 - D_i^2) \\ &+ \frac{1}{6} \cot(\alpha_1) (D_{f1}^3 + 2D_{i2}^3 - 3D_{f1} D_{i2}^2) + \frac{1}{6} \cot(\alpha_2) (D_{f2}^3 + 2D_{i2}^3 - 3D_{f1} D_{i2}^2) \end{aligned} \quad (12)$$

Hypothesizing that: $\alpha_1 = \alpha_2 = \alpha$; $D_{f1} = D_{f2} = D_f$. Blank length expression becomes (13)

$$L_1 = \frac{D_f^2 - D_i^2}{D_1^2 - D_i^2} (L_{f1} + L_{f2}) + \left(\frac{D_2^2 - D_i^2}{D_1^2 - D_i^2} \right) L_{i2} + \frac{1}{3} \cot(\alpha) \left(\frac{D_f^3 + 2D_{i2}^3 - 3D_f D_{i2}^2}{D_1^2 - D_i^2} \right) \quad (13)$$

As in the inverse expression (8), D_1 could be derived as in (14).

$$D_1 = \left(\frac{(L_{f1} + L_{f2})(D_{f2}^2 - D_i^2) + L_2(D_{i2}^2 - D_i^2) + \frac{1}{6} \cot(\alpha)(D_{f1}^3 + 2D_2^3 - 3D_{f1}D_2^2)}{L_1} + D_i^2 \right)^{\frac{1}{2}} \quad (14)$$

If two (or more) consecutive flanged pipes needed to be realized, second term of (12) should be multiplied for two (or more).

Appendix 3. S/L ratio

Expression of circumferential contact (S) and axial contact (L), from Gur and Tirosch (1982).

$$S = R_R \beta \quad (15)$$

$$L \cong \left(\frac{T_0 - T_f + 2}{f + \tan \alpha} \right) \quad (16)$$

where: $\beta = \cos^{-1} \left(\frac{a^2 + c^2 - b^2}{2ac} \right)$; $a = R_R + T_{fi} + R_M$; $b = R_M + T_{fi} + f \tan \alpha$; $c = R_R$. With, R_D , roller radius (mm); R_M , mandrel radius (mm); α , roller attack angle; T_0 , initial thickness (mm) T_f final thickness (mm).

Appendix 4. Energy based flow model

Equation (8) describes the total flow forming energy (U_e), as in Hayama and Kudo (1979a).

$$U_e = U_f + U_b = (U_{if} + U_a + U_{ff} + U_r) + (U_{ib} + U_{fb}) \quad (17)$$

Referring to Figure A3, every energy contribute can be described as follows: U_p energy consumed in ranges of $z > 0$; U_b , energy consumed in ranges of $z < 0$; U_{if} , plastic deformation energy under roller for $z > 0$; U_{ib} , plastic deformation energy under roller for $z < 0$; U_a , plastic flow velocity discontinuity energy on roller entrance (HE'); U_{ff} frictional energy consumed on contact surface between roller/blank and blank mandrel for $z > 0$; U_{fb} , frictional energy consumed on contact surface between roller/blank and blank mandrel for $z < 0$; U_r , plastic flow velocity discontinuity energy on roller exit (EL). Applied forming powers and forces equations are developed from Equation (17), they can be found in (Hayama & Kudo, 1979a, 1979b; Jolly & Bedi, 2010; Marini, Cunningham, & Corney, 2014; Singhal et al., 1990).

Contact surface area need to be calculated trough definition of $z_g(z > 0)$ and $z_n(z < 0)$. Referring to Figure A3, the first was defined as a parabola passing for vertex $E = (0, z_E)$ and point $E' = (x_a, z_{E'})$. The second was similarly defined but passing for vertex $E = (0, z_E)$ and point $E' = (x_a, z_{E'})$. Consequently,

$$z_g = \frac{z_{E'} - z_E}{x_a^2} x^2 + z_E \quad (18)$$

$$z_n = \frac{z_L}{x_b^2} x^2 + z_L \quad (19)$$

Thus, contact surface were defined as follows and calculated using (18) and (19).

$$S_f = \int_0^{x_a} z_g dx = \frac{z_{E'} - z_E}{3} x_a + z_E x_a \quad (20)$$

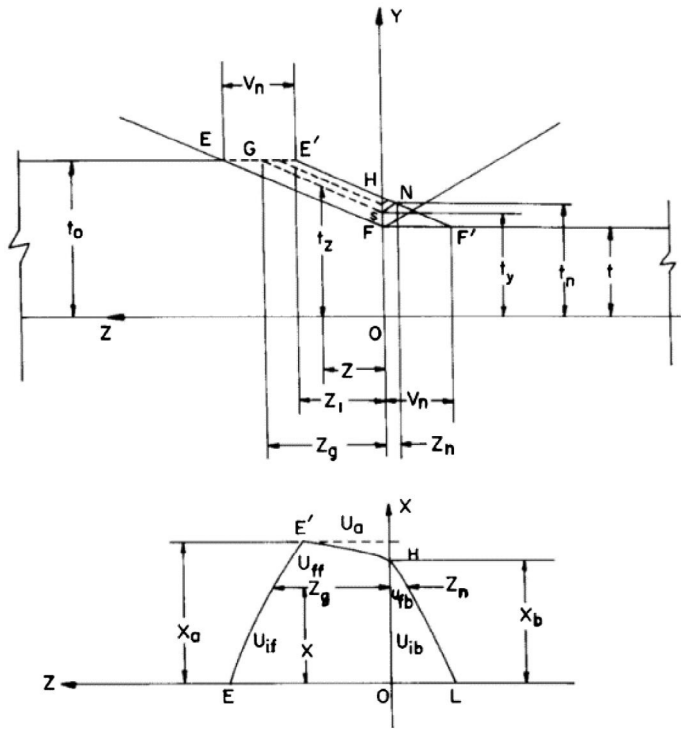


Figure A3. Energy method, contact zone model for flow forming (Hayama & Kudo, 1979a).

$$S_b = \int_0^{x_b} z_n dx = \frac{4}{3} z_L x_a \tag{21}$$

Radial force (P_r) contributes in $z > 0$ and $z < 0$ were described as follows.

$$P_{rf} = \frac{U_f}{Y_f} S_f \tag{22}$$

$$P_{rb} = \frac{U_b}{Y_b} S_b \tag{23}$$

Consecutively, the total radial forces (y -axis)

$$P_r = P_{rf} + P_{rb} \tag{24}$$

The axial force (z -axis)

$$P_z = P_r \tan(\alpha) \tag{25}$$

Appendix 5. Time and cost models

Time model (flow-turning model). Referring to Figure 9, forming lengths (green) and transverse lengths (red) could be identified for every flow forming pass (i -th)

$$L_{\text{forming,pass-}i} = \sum_{K=1}^{N_o} L_{Ok} \tag{26}$$

$$L_{\text{transverse,pass-}i} = \sum_{K=1}^{N_T} L_{TK} \quad (27)$$

For i -th flow forming pass: $L_{\text{forming,pass-}i}$ (26), total formed length i -th pass; $L_{\text{transverse,pass-}i}$ (27), total transverse length; L_{Ok} , k -th formed length; L_{Tk} , k -th transverse length for i -th pass, N_o , number of forming length sections, N_T , number of transverse length sections.

$$t_{\text{forming,pass } i} = \frac{F_{\text{pass-}i}}{L_{\text{forming,pass } i}} \quad (28)$$

$$t_{\text{transverse,pass } i} = \frac{v_{\text{pass-}i}}{L_{\text{transverse,pass } i}} \quad (29)$$

For i -th flow forming pass, $t_{\text{forming,pass } i}$ (28), total forming time, $t_{\text{transverse,pass } i}$ (29), total transverse time, $F_{\text{pass-}i}$, feed rate in mm/min, $v_{\text{pass-}i}$, transverse speed in mm/min. Total operative time in $t_{\text{operative,pass } i}$ is expressed as in (30).

$$t_{\text{operative,pass } i} = t_{\text{forming,pass } i} + t_{\text{transverse,pass } i} \quad (30)$$

Hybrid cost model. Cost model was created in order to calculate manufacturing cost, derived from (Allen & Swift, 1990; Kalpakjian & Schmid, 2009; Swift & Booker, 2013). Only direct costs were involved in calculation. (i.e. costs directly imputable to process). Total cost expression (15) includes labor cost (35), material cost (16), tool cost (37), working operative cost (36) as variable costs. Machine depreciation (39) and maintenance cost (40) has been considered as constant. Indirect costs were not considered in this investigation. By the way, usual general cost formula could be written as follows

$$C_{\text{Total/piece}} = C_{\text{Direct-Variable}} + C_{\text{Direct-Fixed}} + C_{\text{Indirect}} \quad (31)$$

$$C_{\text{Direct,Variable}} = C_{\text{Material}} + C_{\text{Labor}} + C_{\text{Tool}} + C_{\text{Working}} \quad (32)$$

$$C_{\text{Material}} = V_{\text{preform}} \rho c_{\text{material}} \quad (33)$$

With, C_{Material} , total material cost, V_{preform} , preform volume (mm^3) ρ , material density (kg/mm^3), c_{material} , material cost ($\text{£}/\text{kg}$).

Flow forming process has been as composed of five main phases: $t_{\text{set-up}}$, set-up time, machine programming in order to absolve the task (machine stopped, idle machine time); t_{load} , part loading time, workpiece clamping on the machine (machine stopped, idle machine time); t_{FFP} , forming time, divided in preliminary operations ($t_{(\text{pre,ops})i}$) ending operation ($t_{(\text{end-ops})i}$) and working time ($t_{(\text{operative})i}$) (machine working, idle worker time); part unloading, released worked part from the machine (machine stopped, idle machine time); t_{Qcheck} , quality check time, assigned only to a fixed sample of pieces (not idle time, in parallel with other operations). Usually flow forming pieces did not need change clamping references during operations, so, forming pass can be done consecutively (Figure A4).

Total time flow forming, including quality check, can be written as in (34).

$$t_{\text{total/piece}} = t_{\text{set-up}} + \sum_{i=1}^{n-\text{passes}} \left(t_{(\text{load})i} + t_{(\text{unload})i} + t_{(\text{pre,ops})i} + t_{(\text{operative})i} + t_{(\text{end-ops})i} \right) + t_{\text{Qcheck}} \quad (34)$$

Consecutively, labor cost could be defined as (35).

$$C_{\text{Labor}} = C_{\text{skilled worker}} + C_{\text{unskilled worker}} \left(t_{\text{set-up}} + t_{\text{load}} + t_{\text{unload}} + t_{\text{FFI}} + t_{\text{Qcheck}} \right) \quad (35)$$

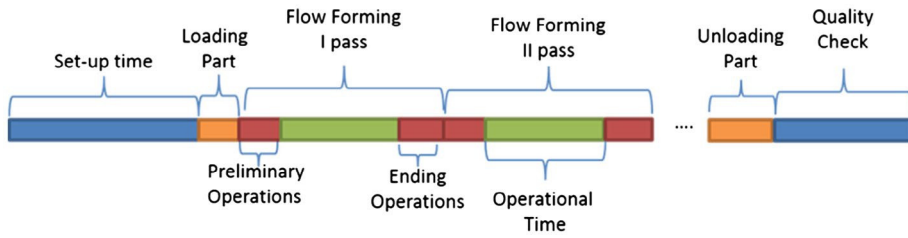


Figure A4. Flow forming process time model schematization.

With, C_{Labour} , total labor cost (£); c_{labour} , labor cost per min (£/min); t_{set-up} , set-up time (min); t_{FFP} , forming time (min); t_{unload} , unloading time (min); t_{load} , loading time (min); t_{check} , quality check time (min).

Forming operation cost can be formulated as in (36)

$$C_{Working} = \sum_{i=1}^{n-passes} (W_{forming-i} + W_{transverse-i}) c_{energy} t_{FFi} \tag{36}$$

With, $C_{Working}$, total working cost (£); $W_{forming-i}$, forming power calculated through the energy based model (Appendix 4); $W_{transverse-i}$, machine transverse energy, considered as ($W_{transverse} = 0.01 W_{forming}$); c_{energy} , energy cost (£/W).

Tools cost could be written as follows, giving a rough estimation of tool life (37).

$$C_{Tool} = C_{single\ tool} \frac{T_{tool\ life}}{(t_{op1} + \dots)} \tag{37}$$

C_{Tool} , tool cost imputable to flow forming operation (£); $C_{single\ tool}$, single tool set cost (£); $T_{tool\ life}$, medium tool life (min); $\frac{T_{tool\ life}}{(t_{op1} + \dots)}$, portion of tool life used by process (%). Fixed costs were assigned to all the process because they were specifically not assigned to a single operation, as in (38).

$$C_{Direct, Fixed} = C_{Machine\ Depreciation} + C_{Maintenance} + \dots \tag{38}$$

Machine depreciation is defined as in (39) (Kalpakjian & Schmid, 2009),

$$C_{Machine\ Depreciation} = C_{Machine} \frac{t_{total/piece}}{y_{depreciation} d_{working} h_{working} 60} \tag{39}$$

With, $C_{Machine\ Depreciation}$, depreciation cost (£); $C_{Machine}$, total machine cost (£); $t_{total/piece}$, lead-time (min); $y_{depreciation}$, machine fixed depreciation years (years); $d_{working}$, machine working days per year (days/year); $h_{working}$, machine working hours per day (min/days). Maintenance cost (40) can be expressed as a part of the machine depreciation (39).

$$C_{Maintenance} = 0.07 C_{Machine\ Depreciation} \tag{40}$$